

# Resilient Consensus Against Epidemic Malicious Attacks

Yuan Wang, *Member, IEEE*, Hideaki Ishii, *Fellow, IEEE*,  
François Bonnet, and Xavier Défago, *Member, IEEE*

**Abstract**—This paper addresses novel consensus problems for multi-agent systems operating in a pandemic environment where infectious diseases are spreading. The dynamics of the diseases follows the susceptible-infected-recovered (SIR) model, where the infection induces faulty behaviors in the agents and affects their state values. To ensure resilient consensus among the noninfectious agents, the difficulty is that the number of infectious agents changes over time. We assume that a high-level policy maker announces the level of infection in real-time, which can be adopted by the agents for their preventative measures. It is demonstrated that this problem can be formulated as resilient consensus in the presence of the so-called mobile malicious models, where the mean subsequence reduced (MSR) algorithms are known to be effective. We characterize sufficient conditions on the network structures for different policies regarding the announced infection levels and the strength of the pandemic. Numerical simulations are carried out for random graphs to verify the effectiveness of our approach.

**Index Terms**—Fault tolerant distributed algorithms, multi-agent systems, resilient consensus, epidemic malicious model.

## I. INTRODUCTION

Recently, the pandemic of COVID-19 has highlighted the necessity and effectiveness of unknown disease peak control. Since it may take up to several years to develop and supply vaccines sufficiently broadly [8], a large ratio of population may become infected simultaneously, which would cause huge pressure to hospitals and medical sectors. Initial measures such as keeping social distance and avoiding unnecessary gatherings are introduced to slow down the disease spreading. By temporarily reducing contacts with others at proper periods, peaks can be reduced in frequency and the number of infected patients. Recent studies related to theoretical studies on peak control can be found in, e.g., [12], [18].

In this work, we formulate a novel problem in the context of resilient consensus for multi-agent systems, where the agents may fall in infectious statuses depending on the susceptible-infected-recovered (SIR) epidemic dynamics in the environment. Infected agents will take unexpected behaviors in their values and agents free from the disease should avoid using such state values when updating their own ones. While

we follow the line of research on fault tolerant consensus algorithms (e.g., [13]), the main difference is that the number of fault agents is time varying. This information may be partially known from high-level policy makers who attempts to estimate the epidemic condition and make announcement about it in real time.

It is emphasized that to deal with this problem, the notion of mobile malicious agents studied in [32] becomes critical. Inspired by epidemic peak control [12], [18], we extend the mobile malicious model to the case with pandemic behaviors. Here, the malicious agents no longer move, but may infect other regular agents. For the infected agents, their behaviors as well as their values can be changed. Meanwhile, the infected agents will also recover after the infection at a certain rate. Once cured, they should follow the designed update rules even if their own values may be corrupted.

We note that the SIR epidemic model used in this paper represents the disease dynamics of large population. The agent network is a small part of the population and thus does not affect the infection model. Moreover, a well-mixed, homogeneous infection condition is assumed so that for the neighbors of each agent, the infected ratio is upper bounded by the general infection ratio. At the agent level, when an agent is infected, its value becomes strange and corrupted. Exchanging values with infected neighbors does not induce infections, but when one uses values from infected agents, the agent may take a corrupted value as well.

*Related works:* Epidemic models have been long studied among many different fields including mathematical biology [11], computer science [21], social science [10] and so on. Different epidemic models have been studied in the literature, but the most common ones include the susceptible-infected-susceptible (SIS) model and the SIR model. In the traditional SIS model, the population is divided into two groups taking the susceptible and infected states; the ratios of the two groups may exhibit dynamic behaviors over time. More recently, the SIS model incorporates networks representing interactions of agents, where the pandemic process evolves over time-varying networks [22], [23], [30]. Similar trends can be found in the SIR model, where the agents may be in susceptible, infected, or recovered state. Once agents are recovered from their infected states, they will not be infected again. Recent works on SIR-type models focus on improving the model based on real data [5], considering time delay issues [3], and applying the SIR model in other problems such as information source detection [6] and information epidemics in social networks [15]. In [19], the development, analysis and control problems for epidemic models are reviewed from the viewpoint of systems control.

This work was supported in part by the JSPS under Grant-in-Aid for Scientific Research Grant No. 18H01460. The support provided by the China Scholarship Council is also acknowledged.

Y. Wang is with the Division of Decision and Control Systems, KTH Royal Institute of Technology, Stockholm, Sweden. H. Ishii, F. Bonnet and X. Défago are with the Department of Computer Science, Tokyo Institute of Technology, Tokyo/Yokohama, Japan. E-mails: wang.y.bb@m.titech.ac.jp, {ishii,bonnet,defago}@c.titech.ac.jp

The works such as [11], [12], [18] mainly focus on the ratio of infectious dynamic which is based on a large amount of individuals. In order to explain the spreading process in networks, multiple stochastic models are proposed. One line is to model it by Markov theory [1], [2], [16], [17], [20], [25], [26], [31], [34]. Among such spreading models, the majority of the works discusses the SIS epidemic process and attempts to reach disease-free equilibrium (DFE), which means the equilibrium point without infections. In order to reach DFE, the curing rate in the network should be high. In particular, the basic reproduction number in the network needs to be less than or equal to one [17]. The pandemic and recovery speeds are determined by contact network structure. By minimizing the spectral norm of the transition matrix, the epidemic spreading process can be suppressed [16], [25], [31]. Moreover, by combining the protection resources such as vaccines or antidotes, the cost-optimal resources distribution problem is studied in SIS [25] and SIR [20] processes. In [34], the typical SIS process is extended to Susceptible-Exposed-Infected-Vigilant (SEIV) epidemic process. A model predictive controller is proposed to extinct the SEIV process, meanwhile, minimizing the control resource cost.

Other studies about epidemic processes, such as network reconstruction problem [24], aim to estimate a contact network from the viral observations in groups of individuals. Game formation approach is a tool to study the human decision making during the SIS epidemic process in networks [9], [14], [27], [28]. The basic idea is that the agents in the network can protect itself or recover with some cost. Then there are investment games and the need to find proper protection strategies. To study the social optimal vaccination policy, a population game framework is formulated and decentralized protection strategies are studied in [9]. In [14], a zero-determined strategy is proposed into the vaccination game, to optimize the social costs.

In this work, we follow the line of fault-tolerant algorithms for multi-agent systems. Suppose that the infected agents follow the so-called *malicious adversary model*. The infected agents may lose their original state values and broadcast their corrupted values. The goal for other non-infected agents is to reach consensus at a safe value, within the range of the original values of the non-infectious agents. Moreover, our results are motivated by the class of Mean Subsequence Reduced (MSR) algorithms, which has been studied in [13], [29], [32]. In such algorithms, the non-infected agents ignore suspicious values from their neighbors. Such algorithms do not need to detect the adversarial neighbors, but require a certain level of connectivity in the network.

**Contributions:** The contribution of this work is threefold: First, we extend the mobile adversary model of one-to-one mobile behavior to an epidemic case. In our previous work [32], a malicious agent moves to another agent and leaves a corrupted value. The agent that just recovered is considered as a cured agent. Note however that such an agent may have a corrupted value and hence should be treated as a malicious one for another round so as to apply a protocol to adjust its value. Second, we introduce an intervention measure to the epidemic model to enhance the resiliency of the consensus protocols

employing the modified MSR algorithms. In conventional epidemic works such as [18], the intervention takes the form of the ratio at which the general public should avoid contacts with others. In this work, we relate such intervention ratio with the parameters employed in MSR algorithms for pruning the neighbors' values; we formally analyze their role in resilient consensus. Third, based on the modified MSR algorithms used for mobile malicious models, we propose two protocols with static and adaptive policies for the intervention ratio globally announced and hence the the pruning parameters locally at the agents. For both protocols, we characterize the graph conditions and tolerable pandemic level under which resilient consensus can be guaranteed. Compared with the conventional mobile malicious model, the epidemic malicious model is more powerful since it has dynamic malicious agents. The pruning number is no longer given, but has to be chosen properly according to the infection level at the time. The existence of pruning numbers that can guarantee resilient consensus in a given graph is also discussed.

**Outline:** This paper is organized as follows. In Section II, preliminaries and the general problem setting are introduced. In Section III, two protocols for resilient consensus are proposed based on static and realtime information regarding the infection. Our results for complete and noncomplete graphs are presented in Sections IV and V, respectively. We demonstrate the efficacy of the algorithms by numerical examples in Section VI. Section VII gives concluding remarks. A preliminary version of this paper will appear as a conference paper [33]. The current paper contains all proofs for theoretical results and extensive simulation results are carried out as well.

## II. PROBLEM FORMULATION

### A. Preliminaries on Graphs

Denote by  $\mathcal{G} = (\mathcal{V}, \mathcal{E})$  the graph consisting of  $n$  nodes, where  $\mathcal{V} = \{1, 2, \dots, n\}$  is the set of nodes and  $\mathcal{E} \subset \mathcal{V} \times \mathcal{V}$  is the set of edges. The edge  $(j, i) \in \mathcal{E}$  indicates that node  $j$  can send a message to node  $i$  and is called an incoming edge of node  $i$ . Directed graphs are considered, in which  $(j, i) \in \mathcal{E}$  does not necessarily imply  $(i, j) \in \mathcal{E}$ . Let  $\mathcal{N}_i = \{j : (j, i) \in \mathcal{E}\}$  be the set of in-neighbors of node  $i$ . The in-degree  $d_i$  of node  $i$  indicates the number of its in-neighbors, i.e.,  $d_i = |\mathcal{N}_i|$ .

The path from node  $i_1$  to node  $i_p$  is denoted as the sequence  $(i_1, i_2, \dots, i_p)$ , where  $(i_j, i_{j+1}) \in \mathcal{E}$  for  $j = 1, \dots, p-1$ . The graph  $\mathcal{G}$  is said to contain a spanning tree if from some node, there are paths to all other nodes in the graph.

### B. Overall System Model

In this subsection, we provide an overview of the problem setting of resilient consensus for multi-agent systems in an environment where diseases are spreading.

The overall system considered here consists of two layers, representing different models related to (i) the environment and (ii) multi-agent systems. The framework of the overall system is shown in Fig. 1. In the first layer, there are policy makers in charge to estimate the ratio of the infectious population and then to announce how everyone in the system

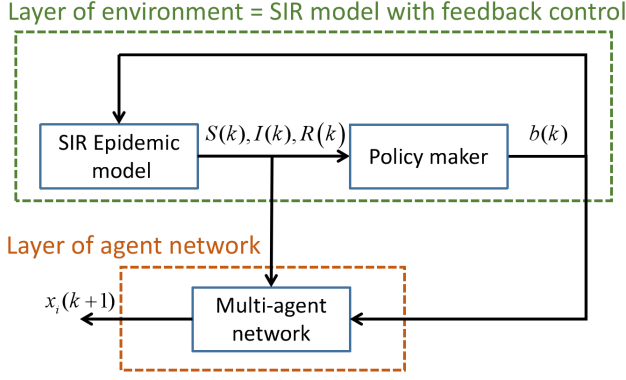


Fig. 1. Overall system model

should reduce their interactions with others. The announcement is made by adjusting the so-called *reduction parameter*. This provides a feedback control mechanism to suppress the infection peak in the SIR epidemic model.

The second layer is at the lower level, containing a number of agents represented by a network. They are placed in the environment, which is dominated by the disease dynamics of a large population. The dynamics is represented by the standard SIR epidemic model, which determines the proportions of the population susceptible, infectious, and recovered, and hence the agents are subject to infections. However, the agents' behaviors do not affect the environment since the population is much larger. On the other hand, it is assumed that the agents are infected in a homogeneous manner. This means that for each agent, the ratio of infectious agents among the neighbors strictly follows that of the population. We will later explain these points more.

Furthermore, in the second layer, the regular agents in the susceptible and recovered states employ a resilient variant of consensus protocols called the MSR algorithms. The agents will follow the announced level of reduction parameter from the policy maker. Specifically, they reduce their contacts by ignoring some of the values received from neighbors. Notice that due to the SIR epidemic model, the number of neighbors who may be infectious is time varying. In particular, the recovered agents have to be careful not to restart their consensus protocols using the values from the infected periods. Under such circumstances, conventional resilient consensus algorithms are not capable to eliminate the adversarial effects. Instead, one must resort to the notion of mobile adversarial models, where the identities of the malicious agents switch, and also to algorithms robust to such models (e.g., [4], [7], [32]).

The objective of the multi-agent system in the lower layer is to reach consensus on their state values, and this must be achieved without being influenced by the infected agents. The susceptible agents do not become infected by solely interacting with infectious agents. However, the states of the infectious agents may be affected by the disease. Thus, the susceptible and recovered agents must take preventative measures at the time of updating their own state values.

In our problem setting, three issues are present, creating difficulties for the decision making of the agents to reach consensus. First, the infection may spread quickly depending

on the parameters that determine the strength of the disease spreading, and large peaks may appear. Second, the ratio of infectious population is unknown in general. In the second layer, this means that the identities of the infectious agents are unknown to the susceptible and recovered ones. As a third hurdle, we impose that the agents must continue with their interactions during the high peaks. This is because if sufficiently many agents become infected over time, the original values of their states may become lost from the system, which will make it difficult for the agents to arrive at a safe, reasonable value for consensus. We mention this point since in the SIR epidemic model, the infections are bound to cease in the long run. Hence, the most critical incident that must be avoided is to lose safe values from the entire multi-agent system.

### C. First Layer of the SIR Epidemic Model

In the first layer, to describe the disease spreading, we consider a variant of the standard SIR epidemic model with a policy maker who attempts to regulate spreading of the disease by making announcements so that contacts within the population decreases [18].

In the environment, the fractions of the population susceptible, infectious, and recovered at continuous time are denoted, respectively, by  $S(t)$ ,  $I(t)$ , and  $R(t)$ , where  $S(t) + I(t) + R(t) = 1$  at all  $t$ . In this model, the disease spreads at the transmitting rate  $\beta > 0$  while the infection recovers at the recovering rate  $\gamma > 0$ . It is common to denote the basic reproduction number by  $R_0 = \beta/\gamma$ . It represents the reproduction ability, which may correspond to the strength of the general disease spreading behavior.

The role of the policy maker is to regulate the transmitting rate by forcing the population to reduce their contacts with others. The transmission reduction rate is represented by the parameter  $b(t) \in [0, 1]$  and this results in a smaller transmitting rate at  $b(t)\beta$ . In the common SIR model where no regulation is made, this parameter remains at  $b(t) \equiv 1$ .

With the transmission reduction based on  $b(t)$  at time  $t$ , the pandemic process is described by the SIR model as

$$\begin{aligned}\dot{S}(t) &= -b(t)\beta S(t)I(t), \\ \dot{I}(t) &= b(t)\beta S(t)I(t) - \gamma I(t), \\ \dot{R}(t) &= \gamma I(t).\end{aligned}\tag{1}$$

In this paper, we deal with the system in the discrete-time domain and thus discretize the SIR system model above. Let  $\Delta T$  be the sampling period. Denote the variables at time  $k\Delta T$  by  $S(k)$ ,  $I(k)$ , and  $R(k)$  and so on. Based on the Euler method, when  $\Delta T$  is sufficiently small, the continuous-time dynamics in (1) can be approximately described by the following discrete-time dynamics:

$$\begin{aligned}S(k+1) &= S(k) - b(k)\beta S(k)I(k)\Delta T, \\ I(k+1) &= I(k) + b(k)\beta S(k)I(k)\Delta T - \gamma I(k)\Delta T, \\ R(k+1) &= R(k) + \gamma I(k)\Delta T.\end{aligned}\tag{2}$$

As mentioned above,  $b(k)$  is the key parameter to control the pandemic peak. It is determined by the policy maker who performs the analysis on  $I(k)$ .

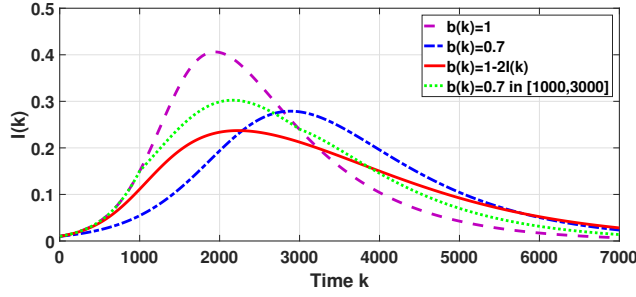


Fig. 2. Infectious ratio  $I(k)$  under different control policies

Different policies can be considered for the choice of the transmission reduction. We illustrate this point by a numerical example with the basic parameters taken as  $\beta = 0.4$ ,  $\gamma = 0.1$ , and  $\Delta T = 0.01$ . In Fig. 2, the time responses of the infectious ratio  $I(k)$  are shown under four policies: (i) The base case with no reduction (i.e.,  $b(k) \equiv 1$ ) in dashed line, (ii) fixed reduction at  $b(k) \equiv 0.7$  in dash-dot line, (iii) adaptive reduction  $b(k) = 1 - 2I(k)$  with the knowledge of the infectious rate  $I(k)$  in solid line, and (iv) reduction at limited time period based on  $b(k) = 0.7$  for  $k \in [1000, 3000]$  and 1 otherwise in dotted line. The initial states are taken as  $S(0) = 0.99$ ,  $I(0) = 0.01$ , and  $R(0) = 0$ .

Notice that in the base case (i), the transmitting rate  $\beta$  is high, resulting in the peak of  $I(k)$  greater than 0.4. In the other cases, the peaks are about 0.3. The simple policy (ii) with  $b(k) \equiv 0.7$  is the most demanding in terms of transmission reduction over time; the peak is smaller than 0.3, but occurs late, delaying the recovery. The adaptive policy (iii) is also demanding, but the reduction increases slowly in response to  $I(k)$ ; the peak is less than 0.25 and occurs early. The time-limited method (iv) is also effective to keep the peak to appear early in time.

### III. LAYER OF THE MULTI-AGENT SYSTEM

In this section, we explain the the lower layer of the overall system, where the multi-agent system is placed.

#### A. Resilient Consensus

The network of agents is represented by the directed graph  $\mathcal{G}$ . In our setting, the status of the agents is determined by the condition of the disease in the environment as follows. At each time  $k$ , in accordance with the fractions of  $S(k)$ ,  $I(k)$ , and  $R(k)$  in the SIR epidemic model, the agent set  $\mathcal{V}$  is partitioned into  $\mathcal{S}(k)$  of susceptible agents,  $\mathcal{I}(k)$  of infectious agents, and  $\mathcal{R}(k)$  of recovered agents, where  $\mathcal{S}(k) \cup \mathcal{I}(k) \cup \mathcal{R}(k) = \mathcal{V}$ .

Each agent  $i \in \mathcal{V}$  has a state value denoted by  $x_i(k)$  at time  $k$ . At nominal times when no outbreak of the disease is present, all agents would follow the protocol below for seeking consensus in their values:

$$x_i(k+1) = \sum_{j \in \{i\} \cup \mathcal{N}_i} a_{ij}(k) x_j(k), \quad (3)$$

where the weights  $a_{ij}(k) \in [0, 1)$  satisfy  $a_{ii}(k) + \sum_{j \in \mathcal{N}_i} a_{ij}(k) = 1$ . It is well known that the agents will arrive at consensus, i.e.,  $|x_i(k) - x_j(k)| \rightarrow 0$  as  $k \rightarrow \infty$  for  $i, j \in \mathcal{V}$  if the network  $\mathcal{G}$  contains a directed spanning tree.

We call the agents to be *regular* if they are in the susceptible status  $\mathcal{S}(k)$  and the recovered status  $\mathcal{R}(k)$ . These agents are capable to execute the given algorithm and maintain their values accordingly. On the other hand, the infected agents may have corrupted values. In particular, for each agent in the infectious status  $\mathcal{I}(k)$ , its value is updated as

$$x_i(k+1) = u_i(k), \quad i \in \mathcal{I}(k), \quad (4)$$

where the input  $u_i(k)$  can be set arbitrarily due to the disease.

Now, we introduce the notion of resilient consensus for the multi-agent system under the epidemic model.

**Definition 3.1: (Resilient consensus)** If for any possible sets and behaviors of the infectious agents and any state values of the regular agents, the following two conditions are satisfied, then we say that the regular agents reach resilient consensus:

- 1) Safety condition: There exists a bounded interval  $\mathcal{B} \subset \mathbb{R}$  determined by the initial states of the regular (susceptible and recovered) agents such that  $x_i(k) \in \mathcal{B}$  for all  $i \in \mathcal{S}(k) \cup \mathcal{R}(k)$ ,  $k \in \mathbb{Z}_+$ .
- 2) Consensus condition: The regular agents eventually take the same value as  $\max_{i,j \in \mathcal{S}(k) \cup \mathcal{R}(k)} |x_i(k) - x_j(k)| \rightarrow 0$  as  $k \rightarrow \infty$ .

In our approach, the regular agents follow the so-called MSR algorithm to protect their values from being corrupted by using those received from infected agents. Their states are updated as in (3), but with a restricted number of neighbor values using the pruning number  $F_i(k) \in [0, d_i/2)$  for  $i \in \mathcal{V}$ . The algorithm is outlined below. In particular, we present a modified version of the MSR algorithm from [32].

**Algorithm 3.1:** At each round  $k$ , each regular agent  $i \in \mathcal{S}(k) \cup \mathcal{R}(k)$  executes the following three steps:

- 1) Agent  $i$  sorts the values  $x_j(k)$ ,  $j \in \mathcal{N}_i$ , received from its neighbors and its own value  $x_i(k)$  in descending order.
- 2) After sorting, agent  $i$  deletes the  $F_i(k)$  largest and the  $F_i(k)$  smallest values. The deleted data will not be used in the update. The set of indices of agents whose values remained is written as  $\mathcal{M}_i^+(k) \subset \{i\} \cup \mathcal{N}_i$ .
- 3) Finally, agent  $i$  updates its value by

$$x_i(k+1) = \sum_{j \in \mathcal{M}_i^+(k)} a_{ij}(k) x_j(k). \quad (5)$$

For the MSR algorithm to prevent the corrupted values from affecting the agents, it is critical that the regular agents have sufficient information regarding the local infections. In particular, the pruning number  $F_i(k)$  must be greater than the number of infected neighbors at all  $k$  as

$$F_i(k) \geq |\mathcal{N}_i \cap \mathcal{I}(k)|, \quad i \in \mathcal{S}(k) \cup \mathcal{R}(k). \quad (6)$$

Note however that the exact information of  $\mathcal{I}(k)$  is not available to anyone. In our approach, we connect the pruning number  $F_i(k)$  used in the MSR algorithm and the transmission reduction parameter  $b(k)$ . This point is discussed in the next subsection.

#### B. Infectious Rate and Transmission Reduction

As mentioned earlier, we assume that the infection is homogeneous in the population. This means that given the

infectious ratio  $I(k)$ , for each agent  $i$ , the number of malicious neighbors is bounded by  $d_i I(k)$  as

$$|\mathcal{N}_i \cap \mathcal{I}(k)| \leq d_i I(k), \quad i \in \mathcal{V}. \quad (7)$$

On the other hand, the policy makers in the first layer have an estimate of the ratio  $I(k)$  of infectious population and decide the transmission reduction parameter  $b(k)$ . Since  $1 - b(k)$  represents the ratio of contacts that one should cut down on, we assume that the policy makers can ensure

$$b(k) \in [0, 1 - 2I(k)]. \quad (8)$$

Hence, upon receiving the announced value of  $b(k)$ , to follow the policy makers, the regular agents need to choose their pruning numbers  $F_i(k)$  such that  $2F_i(k)/d_i \geq 1 - b(k)$ . Moreover,  $F_i(k) < d_i/2$  is necessary for agents using the MSR algorithm to have at least one neighbor at each update after the removal of extreme values. Thus,  $F_i(k)$  must be chosen as

$$F_i(k) \in \left[ (1 - b(k)) \frac{d_i}{2}, \frac{d_i}{2} \right), \quad i \in \mathcal{S}(k) \cup \mathcal{R}(k). \quad (9)$$

In fact, by (7) and (8), this implies the bound in (6).

### C. Model for Infectious Agents

Here, we characterise the model for the infectious agents in terms of their behaviors when they are infected and then recovered. The infectious agents are considered to be adversarial in this work. In particular, we follow the malicious model of [13], where the classification is based on their number, locations, and behaviors.

**Definition 3.2: (Malicious agents)** An infected agent  $i \in \mathcal{I}(k)$  is said to be malicious if it can arbitrarily modify its local variables as in (4) and send the same value to all of its neighbors each time a transmission is made.

The motivation for considering malicious agents as defined above comes, for example, from the applications of wireless sensor networks where sensor agents communicate by broadcasting their data.

It is important to notice that under our pandemic model, the identities of the infected, malicious agents change over time. This is in contrast to the conventional models in, e.g., [13], where the malicious agents remain the same. To this end, we must incorporate the more general model known as the mobile malicious agents studied in, e.g., [4], [7].

Under such mobile malicious models, the infectious agents have two properties different from the conventional static model (see Fig. 3). First, a malicious agent may infect regular agents so that their statuses change. While infected, agent  $i \in \mathcal{I}(k)$  broadcasts its corrupted state  $x_i(k)$  (controlled as in (4)) to its neighbors, but then becomes recovered at the recovering rate in the SIR epidemic model. Second, once recovered, agent  $i \in \mathcal{R}(k)$  collects and updates its own as a regular agent. However, in the first round after the recovery, the agent may still possess a corrupted value left from its infected period. Hence, such an agent should be considered still infected and will be said to be in the cured status. Moreover, the agent should refrain from using its own value in the cured status. These aspects will be taken into account in the proposed algorithm.

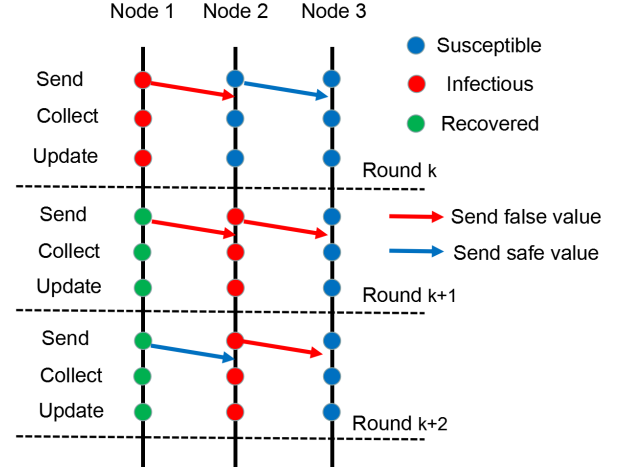


Fig. 3. Epidemic malicious model

### D. Control Policies under the Epidemic Model

In this paper, we address the resilient consensus problem where the agents' statuses change based on the epidemic model. Regarding the transmission reduction parameter  $b(k)$ , two policies are studied: Static and dynamic. The analyses for the two policies will follow in Section IV for the complete graph case and Section V for the noncomplete graph case.

## IV. RESILIENCY RESULTS FOR COMPLETE GRAPHS

We establish conditions under which the agents equipped with Algorithm 3.1 can reach resilient consensus in the epidemic malicious model. In this section, we first present the results for networks in the complete graph form.

The static policy is a special case, where the transmission reduction parameter is fixed as  $b(k) \equiv b_0 \in [0, 1]$  for the entire time horizon. This constraint may limit the feasible strategies for the overall system since the condition in (8) reduces to  $b_0 \leq 1 - 2I(k)$  for all  $k$ . As a consequence, each regular agent  $i$  must use a constant for the number  $F_i(k) \equiv F_{i0}$  of neighbors to be removed as well.

In fact, for this case, an analytic bound for the pandemic peak can be obtained. Suppose that the transmission reduction parameter  $b_0$  is large enough that

$$b_0 R_0 > 1. \quad (10)$$

Note that this relation requires  $R_0 > 1$ . From the work [11], it is known that under these conditions, the maximum of  $I(t)$  in (1) can be obtained as

$$\max_{t>0} I(t) = I(0) + S(0) - \frac{1}{b_0 R_0} \ln S(0) - \frac{1}{b_0 R_0} + \frac{1}{b_0 R_0} \ln \frac{1}{b_0 R_0}.$$

Since  $I(k)$  is the sampled value from (1) and the sampling period  $\Delta T$  is small enough, approximate of the maximum  $I(t)$  can be taken as  $\max_{k \in \mathbb{Z}_+} I(k) \approx \max_{t>0} I(t)$ . Here, for simplicity, we assume that  $S(0) \approx 1$  (and thus  $I(0) \approx 0$ ) and use the upper bound  $I_{\max}(b_0)$  given by

$$I_{\max}(b_0) = 1 - \frac{1}{b_0 R_0} + \frac{1}{b_0 R_0} \ln \frac{1}{b_0 R_0}. \quad (11)$$

Note that if (10) does not hold, i.e.,  $b_0 R_0 \leq 1$ , then the announced transmission reduction parameter is so small

that  $I(k)$  becomes a nonincreasing function of time and thus  $\max_{k \in \mathbb{Z}_+} I(k) = I(0) \approx 0$ . This is a trivial case with no infection and hence not of interest in this paper.

We next introduce a lemma from our previous mobile malicious work [32]. This lemma will be used in the proofs of the results for the complete graph case studied in this section. We slightly modified the statement for the problem setting in this paper.

**Lemma 4.1:** Consider the multi-agent system under the epidemic malicious model with the maximum infectious ratio  $I_{\max}(b_0)$  in (11), whose network  $\mathcal{G}$  forms a complete graph. Then, under (10) the regular agents using Algorithm 3.1 reach resilient consensus if and only if  $n > 2 \max_{i \in \mathcal{V}} F_i(k) + 1 \geq 2I(k)n + 1$ .

#### A. Protocol for the Static Policy

When the policy for the transmission reduction parameter is static, we obtain the following result. Let  $b^*$  be the solution to the equation

$$2I_{\max}(b^*) = 1 - b^*. \quad (12)$$

**Proposition 4.1:** Consider the multi-agent system under the epidemic malicious model whose network  $\mathcal{G}$  forms a complete graph. If  $R_0 > 1$ , then the solution  $b^* \in (1/R_0, 1]$  to (12) always exists. By taking  $b_0 \in (1/R_0, b^*]$  and

$$F_{i0} \in \left[ (1 - b_0) \frac{n-1}{2}, \frac{n-1}{2} \right), \quad (13)$$

the regular agents using Algorithm 3.1 with the static policy reach resilient consensus.

For the complete graph, it holds  $d_i = n - 1$  for all  $i \in \mathcal{V}$ . Thus, from (9), the choice of  $F_{i0}$  becomes that in (13). For later use, let

$$f(b) = 2I_{\max}(b) - (1 - b). \quad (14)$$

*Proof:* We first show that  $b^* \in (1/R_0, 1]$  satisfying (12) always exists. Substituting (11) into  $f(b)$  we have

$$f(b) = 1 + b - \frac{2}{bR_0} + \frac{2}{bR_0} \ln \frac{1}{bR_0}.$$

We discuss the property of  $f(b)$  for  $b \in (1/R_0, 1]$ . Since  $R_0 > 1$ , it is clear that at  $b = 1/R_0$

$$f\left(\frac{1}{R_0}\right) = -\left(1 - \frac{1}{R_0}\right) < 0.$$

Then, at  $b = 1$ , it holds

$$f(1) = 2 - \frac{2}{R_0} + \frac{2}{R_0} \ln \frac{1}{R_0} > 0.$$

In fact,  $f(b)$  is an increasing function in  $(1/R_0, 1]$  since

$$f'(b) = 1 + \frac{2}{b^2 R_0} \ln \frac{1}{bR_0} > 0.$$

Thus, it follows that there always exists  $b^* \in (1/R_0, 1]$  such that  $f(b^*) = 0$  and, moreover, for each  $b \in (1/R_0, b^*]$ , it holds  $f(b) \leq 0$ . This indicates that the chosen  $b_0$  satisfies

$$I_{\max}(b_0) \leq \frac{1 - b_0}{2} < \frac{1}{2}.$$

Hence, we have that  $F_{i0}$  can be taken as in (13). From (13), it is immediate that the conditions in Lemma 4.1 are satisfied. As a result, resilient consensus can be achieved.  $\square$

#### B. Protocol for the Dynamic Policy

Using the dynamic policy for the transmission reduction  $b(k)$ , we can adapt it as the epidemic level changes. The following lemma will be instrumental. It gives an upper bound on the infectious ratio  $I(k)$  under the dynamic policy.

**Lemma 4.2:** Under the epidemic model (2), if the transmission reduction number  $b(k)$  takes the dynamic policy (8), then the maximum infectious ratio meets the relation

$$I(k) < \frac{1}{2} \left( 1 - \frac{1}{R_0} \right) \quad \text{for } k \in \mathbb{Z}_+. \quad (15)$$

*Proof:* By (8), we have  $b(k) \leq 1 - 2I(k)$ . It is clear that the infectious ratio  $I(k)$  is smaller if  $b(k)$  is larger. Hence, we take  $b(k)$  the largest as  $b(k) = 1 - 2I(k)$ . Substituting this into the epidemic model (2), we obtain the dynamics for  $I(k)$  as

$$I(k+1) = I(k) + \beta S(k)I(k)\Delta T(1 - 2I(k)) - \gamma I(k)\Delta T.$$

By the definition of  $R_0$ , this can be written as

$$I(k+1) - I(k) = \beta I(k)\Delta T \left[ S(k)(1 - 2I(k)) - \frac{1}{R_0} \right].$$

Since  $I(k)$ ,  $\Delta T$ , and  $\beta$  are nonnegative, clearly, the sign of the increment  $I(k+1) - I(k)$  is determined by

$$g(k) = S(k)(1 - 2I(k)) - \frac{1}{R_0}. \quad (16)$$

By the assumption  $S(0) \approx 1$ , we have  $I(0) \approx 0$  and thus,  $g(0) \approx 1 - 1/R_0 > 0$ . From (2), if  $b(k) > 0$ ,  $S(k)$  is decreasing. Hence, in the initial period,  $I(k)$  is nondecreasing while  $g(k) \geq 0$ . The value of  $g(k)$  decreases until it becomes negative at some time  $k_1 > 0$ . That is, it holds that  $g(k) \geq 0$  for  $k \in [0, k_1 - 1]$  and  $g(k_1) < 0$ . Then, by (16),

$$I(k_1) = \max_{k \in [0, k_1]} I(k) \leq \frac{1}{2} - \frac{1}{2R_0 S(k_1)} < \frac{1}{2} - \frac{1}{2R_0}.$$

Now, we look at  $I(k)$  for  $k > k_1$ . Suppose that at some time  $k_2 > k_1$ , we have  $I(k_2) \geq I(k_1)$ . From (16), we have

$$\begin{aligned} g(k_2) &= S(k_2)(1 - 2I(k_2)) - \frac{1}{R_0} \leq S(k_2)(1 - 2I(k_1)) - \frac{1}{R_0} \\ &\leq S(k_1)(1 - 2I(k_1)) - \frac{1}{R_0} = g(k_1) < 0. \end{aligned}$$

Hence, it holds  $g(k_2) < 0$  and thus  $I(k_2) < 1/2 - 1/(2R_0)$ . Therefore, for all  $k$ , we attain  $I(k) < 1/2 - 1/(2R_0)$ .  $\square$

We finally characterize conditions for resilient consensus.

**Proposition 4.2:** Consider the multi-agent system under the complete network  $\mathcal{G}$  where the malicious agents follow the SIR epidemic model with  $R_0 > 1$ . If the pruning number satisfies  $I(k) \cdot n \leq F_i(k) < n/2$  for  $i \in \mathcal{S}(k) \cup \mathcal{R}(k)$ , then Algorithm 3.1 with the dynamic policy can guarantee resilient consensus.

*Proof:* Lemma 4.2 shows in particular that under the dynamic policy (8) for  $b(k)$ , it holds  $I(k) < 1/2$  at all times. This is in fact critical for the policy to maintain  $b(k) \geq 0$ . Moreover, the pruning number  $F_i(k)$  can always be selected as in (9). It is then straightforward to show that the conditions in Lemma 4.1 hold. As a result, we conclude that resilient consensus is established.  $\square$

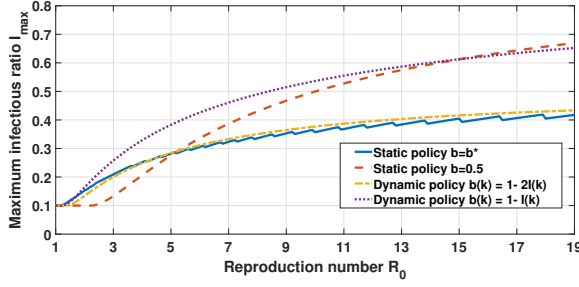


Fig. 4. The maximum infectious ratio  $I_{\max}$  versus reproduction number  $R_0$  under different policies

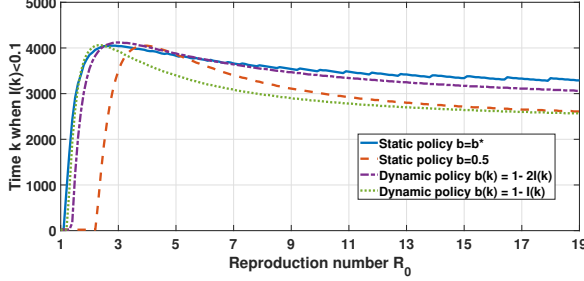


Fig. 5. The time when  $I(k) < 0.1$  versus reproduction number  $R_0$  under different policies

### C. Discussion for the Proposed Two Policies

To compare the two proposed policies, we test them in a range of  $R_0 \in [1, 19]$ , where initial states are set as  $S(0) = 0.9, I(0) = 0.1, \Delta T = 0.01, \gamma = 0.1$ . Moreover, we change the infectious rate  $\beta \in [0.1, 1.9]$  and observe how the maximum infectious ratio changes. The result can be found in Fig. 4. We can see that both proposed policies can suppress the maximum infectious under 0.5 for all  $R_0 \in [1, 19]$ . The other policies such as fixed reduction  $b = 0.5$  or relaxed dynamic policy  $b(k) = 1 - I(k)$  cannot guarantee the maximum infectious under 0.5 when  $R_0$  becomes large. This indicates that our proposed policies are well-designed and the infection ratio could be suppressed as a minor part during the whole pandemic process.

Next, to check the approximate lengths of the pandemic periods under different policies, we show in Fig. 5 the time when  $I(k) < 0.1$  is reached. From the plots, we can see that for proposed static and dynamic policies, when  $R_0 \in [1, 2]$ , there is a significant increase in the pandemic period. This indicates that a small  $R_0$  may not infect a major part of the agent network. The proposed policies could suppress such weak pandemic processes in a short time with small infectious peaks. When  $R_0 > 3$ , the pandemic period does not change too much as  $R_0$  increases. The reason is that the pandemic is so powerful that the infectious agents increase rapidly, and then the susceptible agents decrease rapidly so that the pandemic cannot continue for long. With the same recovering rate  $\gamma$ , they will have similar pandemic periods since the infectious peaks decrease at the same speed. Note that with fixed reduction  $b = 0.5$ , there is a delay in the increase in the pandemic period. In particular, when  $bR_0$  becomes greater than 1, a significant change happens.

## V. RESILIENCY RESULTS FOR NONCOMPLETE GRAPHS

In this section, we demonstrate that for agents operating over a noncomplete graph in the epidemic environment, resilient consensus can be attained by the proposed algorithm. Again, both static and dynamic policies are considered, and we derive conditions on network structures.

In the noncomplete graph case, the pruning number  $F_i(k)$  for  $i \in \mathcal{V}$  should be taken slightly differently from (9) as

$$F_i(k) \in \left[ (1 - b(k)) \frac{n}{2}, \frac{d_{\min}}{2} - \frac{n}{4} \right], \quad i \in \mathcal{V}, k \in \mathbb{Z}_+, \quad (17)$$

where  $d_{\min} = \min_{i \in \mathcal{V}} d_i$ .

For the noncomplete graph case, a sufficient condition on graph structures is provided in [32], which we state as a lemma.

**Lemma 5.1:** Consider the multi-agent system under the epidemic malicious model. Then, the regular agents using Algorithm 3.1 with the dynamic policy and (17) reach resilient consensus if the following condition holds:

$$d_{\min} > 2 \max_{i \in \mathcal{V}} F_i(k) + \frac{n}{2} \geq 2I(k)n + \frac{n}{2}. \quad (18)$$

### A. Protocol for the Static Policy

We demonstrate the effectiveness of the static policy for the noncomplete graph case and provide a condition on the graph structure for achieving resilient consensus under the epidemic malicious model.

The design procedure is as follows. First, assume  $R_0 > 1$ . Let  $b^* \in (1/R_0, 1]$  be the solution to (12). Each agent  $i \in \mathcal{V}$  must have sufficiently many neighbors that

$$d_i \in \left( \left( \frac{3}{2} - b^* \right) n, n \right). \quad (19)$$

Note that by the assumption that  $R_0 > 1$ , such  $d_i$  always exists. Here, we further assume that

$$f\left(\frac{3}{2} - \frac{d_{\min}}{n}\right) < 0. \quad (20)$$

Then, take the transmission reduction  $b_0$  satisfying

$$b_0 \in \left( \frac{3}{2} - \frac{d_{\min}}{n}, b^* \right). \quad (21)$$

The pruning number  $F_{i0}$  for agent  $i$  should be taken as in (17) so that

$$F_{i0} \in \left[ (1 - b_0) \frac{n}{2}, \frac{d_{\min}}{2} - \frac{n}{4} \right], \quad i \in \mathcal{V}. \quad (22)$$

The following result ensures that the parameters appearing in the procedure above can always be found and they will enable the agents to form consensus.

**Theorem 5.1:** Consider the multi-agent system under the network  $\mathcal{G}$ , where the malicious agents follow the SIR epidemic model. Then, the regular agents using Algorithm 3.1 with the static policy and the parameters in (19)–(22) reach resilient consensus.

*Proof:* By the choice of  $d_i$  in (19), we have  $3/2 - d_{\min}/n < b^*$ . Hence, the transmission reduction parameter  $b_0$  satisfying (21) can be taken. Moreover, from (21), we have  $1 - b_0/2 < d_{\min}/2n - 1/4$ . This shows that  $F_{i0}$  in (22) is well defined.

Finally, by (20), it holds that  $I_{\max}(b_0) < (1 - b_0)/2$ , indicating that  $F_{i0}$  from (22) satisfies the condition of Lemma 5.1. Therefore, resilient consensus can be achieved.  $\square$

### B. Protocol for the Dynamic Policy

We give the result when the dynamic policy is used for the noncomplete graphs case. Here, we must limit the level of disease spreading by assuming  $R_0 \in (1, 2)$ . Then, each agent  $i \in \mathcal{V}$  takes enough neighbors so that

$$d_i \in \left( \left( \frac{3}{2} - \frac{1}{R_0} \right) n, n \right). \quad (23)$$

Here, due to the condition on  $R_0$ , it holds  $3/2 - 1/R_0 \in (1/2, 1)$  and hence, by (23), we have  $d_i > 2/n$ .

**Theorem 5.2:** Consider the multi-agent system under the network  $\mathcal{G}$  where the malicious agents follow the SIR epidemic model with  $R_0 \in (1, 2)$ . Then, the regular agents using Algorithm 3.1 with the dynamic policy (8) using parameters in (23) reach resilient consensus.

*Proof:* To establish resilient consensus, we must show that the condition in Lemma 5.1 holds. Under the dynamic policy, by Lemma 4.2, it holds  $2I(k) < 1 - 1/R_0$  at all times. Hence, by (23),

$$d_i > \left( 1 - \frac{1}{R_0} \right) n + \frac{1}{2} n > 2I(k)n + \frac{1}{2} n.$$

Thus, the part of the condition (18) in Lemma 5.1 holds. By the choice of  $F_i(k)$  in (17) and the dynamic policy (8), it follows that (18) is satisfied.  $\square$

Note that this result is quite conservative since Lemmas 4.2 and 5.1 have conservatisms. The actual bound for  $R_0$  may be much more relaxed. We will discuss this point by simulations in the next section.

## VI. NUMERICAL EXAMPLE

We illustrate the performance of our proposed protocols under epidemic adversary models by a numerical example.

Networks with 1000 nodes were generated by randomly placing nodes having the communication radius of  $r$  in the area of  $100 \times 100$ . The connectivity requirements are in general difficult to check. The initial number of infected agents is set to 10 so that  $I(0) = 0.01$ ,  $S(0) = 0.99$ , and  $R(0) = 0$ . To ensure the cardinality of the sets  $\mathcal{S}(k)$ ,  $\mathcal{I}(k)$ , and  $\mathcal{R}(k)$  to be integers, we took  $|\mathcal{S}(k)| = \lceil S(k) \cdot n \rceil$ ,  $|\mathcal{R}(k)| = \lceil R(k) \cdot n \rceil$ , and  $|\mathcal{I}(k)| = n - |\mathcal{S}(k)| - |\mathcal{R}(k)|$ . For simplicity, all agents use the same pruning number, denoted by  $F$ . To check the success rate of resilient consensus under different conditions, Monte Carlo simulations were made. Initial states of the non-infectious agents were randomly taken in the interval of  $[0, 1]$ . On the other hand, the infected agents were forced to take negative state values at  $-1$ .

### A. Complete Graph Case

To build complete graphs, we set the communication radius to be large ( $r = 150$ ). Based on Proposition 4.1, we know that for the reproduction number satisfying  $R_0 > 1$ , we can always find  $b_0 \in [1/R_0, b^*)$  so that we can choose  $F \in ((1 - b_0)(n - 1)/2, (n - 1)/2)$  to guarantee resilient consensus. To verify this result, we chose  $R_0 = 200$  and  $F = 499$  and ran 50 Monte-Carlo simulations. In all cases, resilient consensus was achieved. For the dynamic policy, we took  $F(k) = \lceil I(k) \cdot n \rceil$ ; the results also confirmed successful resilient consensus in all 50 simulations.

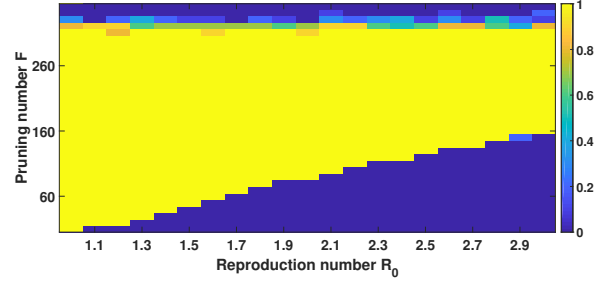


Fig. 6. Static policy: Success rates for resilient consensus versus reproduction number  $R_0$  and pruning number  $F_{i0}$  with parameter  $r = 90$ .

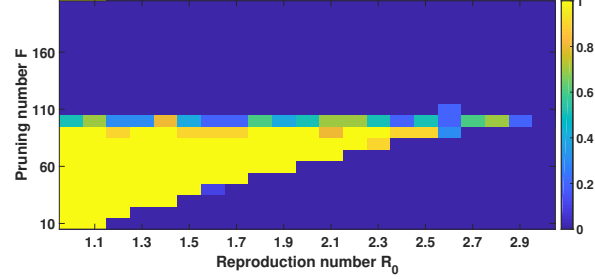


Fig. 7. Static policy: Success rates for resilient consensus versus reproduction number  $R_0$  and pruning number  $F_{i0}$  with parameter  $r = 50$ .

### B. Noncomplete Graph Case

For non-complete graphs, we examined how the parameters  $R_0$ ,  $r$ , and  $F$  affect resilient consensus under the proposed algorithm. First, we focus on the resilience resulting from the network structure. To this end, the communication radii were chosen as  $r = 90$  and  $r = 50$ , which represent dense and sparse networks, respectively. For each pair  $(R_0, F) \in [1, 3] \times [10, 350]$  of the reproduction number and the pruning number, we performed 50 Monte Carlo simulations to find the success rates for resilient consensus.

The results are shown in Figs. 6 and 7 in the form of heatmaps, where colors varying from yellow to blue indicate the success rates from 1 to 0. Fig. 6 shows that in dense networks (with  $r = 90$ ), it is possible to achieve resilient consensus even when the reproduction number  $R_0$  is as large as 3. As the epidemic becomes more powerful with larger  $R_0$ , the yellow area shrinks; the lower bound on  $F$  increases while its upper bound remains about the same. The upper bound of  $F$  is determined by the graph connectivity; when a large pruning number (such as  $F > 320$ ) is used, the network will become too sparse for the MSR to perform properly, leading to failure in reaching consensus.

From Fig. 7, we notice that in sparse networks (with  $r = 50$ ), the yellow area becomes limited in size compared with dense networks (with  $r = 90$ ). (Note however that the scales in  $y$ -axis of the plots are slightly different, and the former is not a subset of the latter.) In particular, resilient consensus is almost impossible for  $R_0 > 2.9$ . The upper bound of pruning number  $F$  for this graph is also much smaller, around 100. Therefore, to summarize, with more connectivity in the network, the multi-agent system can tolerate more powerful epidemics. For sparse networks, resilient consensus may be hard to guarantee and a feasible transmission reduction

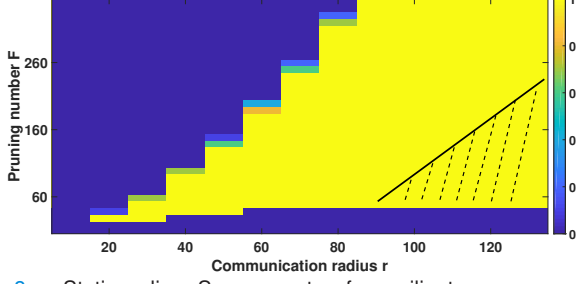


Fig. 8. Static policy: Success rates for resilient consensus versus communication radius  $r$  and pruning number  $F_{i0}$  with parameter  $R_0 = 1.5$ . Shaded area: Approximate pruning number from (22).

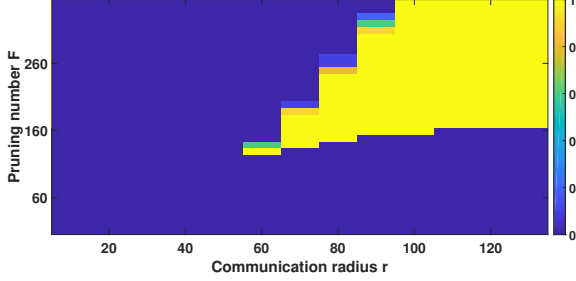


Fig. 9. Static policy: Success rates for resilient consensus versus communication radius  $r$  and pruning number  $F_{i0}$  with parameter  $R_0 = 3$ .

parameter may not exist. These observations are in alignment with the discussions related to Theorem 5.1.

Next, we slightly change our viewpoint and look at the effects of strength in the disease spreading through the reproduction number  $R_0$  on the performance of resilient consensus algorithms. Here, we set  $R_0 = 1.5$  for the weaker case and  $R_0 = 3$  for the stronger case. The success rates for resilient consensus are computed for the pairs  $(r, F) \in [10, 130] \times [10, 350]$  of the communication radius  $r$  and the pruning number  $F$ . Again in the form of heatmaps, the results are shown in Figs. 8 and 9 for  $R_0 = 1.5$  and  $R_0 = 3$ , respectively.

For the results of  $R_0 = 1.5$  in Fig. 8, it is demonstrated that the minimum of the pruning number  $F$  is about 50 while the maximum increases for denser networks with larger radii  $r \geq 40$ . This indicates that in the simulations, the number of infectious agents grew from the initial number of 10 to 50. The shaded area in the plot indicates the bound obtained from (23), exhibiting its conservatism; it shows the necessary radius  $r$  to meet the formula using  $d_{\min}$ .

From the simulation results, if the communication radius reaches  $r = 40$ , we can almost guarantee the success rate to be 1 if  $F = 50$ . However, observe the minimum degree of each agent in this graph, it shows that it is smaller than  $n/2$ . From the theoretical bound of this paper, we need the minimum connection of each agent should reach 600. We confirmed that for  $r \geq 90$ , this condition was guaranteed in the 50 runs. This indicates the difference between the actual bound and the theoretical bound.

Under the stronger epidemics with  $R_0 = 3$ , we can make similar observations from Fig. 9. However, clearly more connectivity is required so that larger values of  $F$  can be used to guarantee resilient consensus. The minimum requirements are roughly  $r \geq 70$  and  $F \geq 150$ .

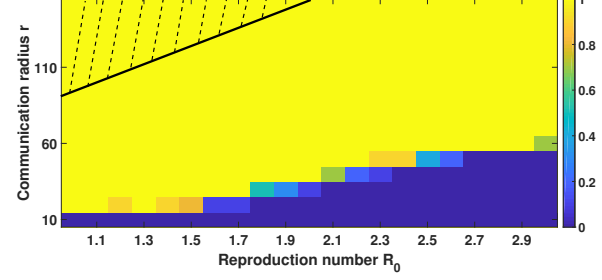


Fig. 10. Dynamic policy: Success rates for resilient consensus versus reproduction number  $R_0$  and communication radius  $r$ . Shaded area: Approximate connection requirement from (23).

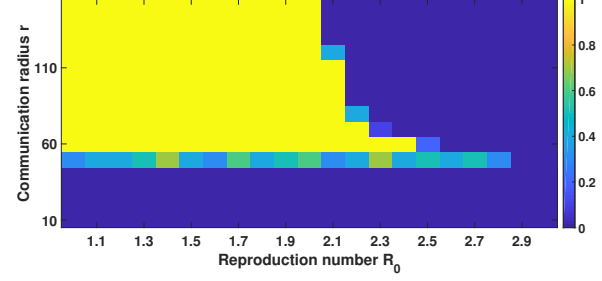


Fig. 11. Static policy without policy maker: Success rates for resilient consensus versus reproduction number  $R_0$  and communication radius  $r$  with  $F_{i0} = 100$ .

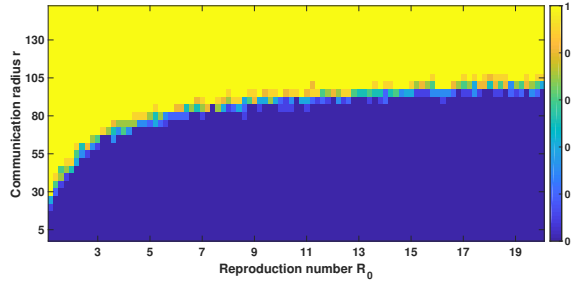
Here, we discuss the performance of the proposed algorithms with dynamic  $F_i(k)$ . Comparisons are made with the static approach using  $F_{i0} = 100$ . The heatmaps representing the success rates of resilient consensus are displayed in Figs. 10 and 11 for  $(R_0, r) \in [1, 3] \times [10, 150]$ .

In comparison, the dynamic policy works well under a range of conditions. This is because the regular agents can adapt their pruning number based on the current infectious level as  $F_i(k) \geq I(k) \cdot n$  guaranteeing  $F_i(k)$  to be always larger than the actual number of infectious agents in realtime. In Fig. 10, observe that as  $R_0$  increases, by choosing denser networks (with larger  $r$ ), the adaptive rule attains resilient consensus. Note that our theoretical result for the dynamic policy guarantees resilient consensus in dense networks with limited  $R_0$ , located in the shaded area at the left top of Fig. 10.

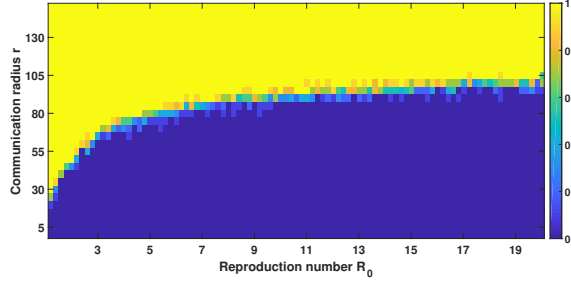
Fig. 11 exhibits the results for the static policy without policy maker where the pruning number is set as  $F_{i0} = 100$ . It is clear by comparing this plot with Fig. 10 that this protocol is much less capable because of the fixed pruning number. The minimum requirement on the radius is  $r = 60$  since each agent must remove 200 values from its neighbors. The advantage of the static policy is that the agents do not need the realtime information of  $b(k)$ . Under mild epidemics with  $R_0 < 2$ , the agents may choose the communication radius  $r \geq 60$ . Then, with  $F_{i0} = 100$ , resilient consensus can be guaranteed.

### C. The Effects of Homogeneous Condition

In this section, we would like to highlight the effects of the homogeneous condition used in the analysis regarding the spreading of disease in the network. We test both static and dynamic policies with homogeneous infected environment and gathered infected environment. In the gathered infected

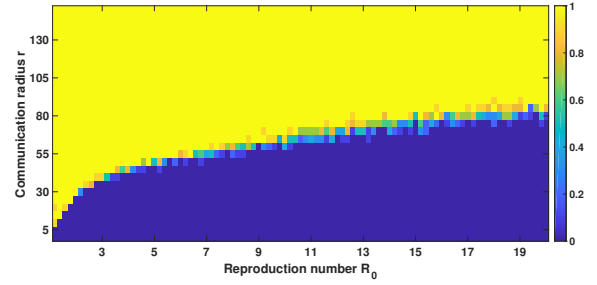


(a) Static policy within homogeneous infection environment

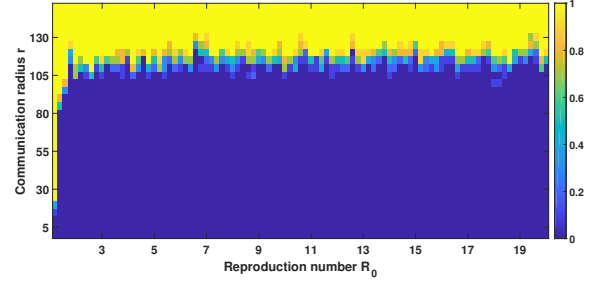


(b) Static policy within gathered infection environment

Fig. 12. Success rates of resilient consensus versus the  $R_0$  of SIR model and  $r$  in the regular agents



(a) Local static policy within homogeneous infection environment



(b) Local static policy within gathered infection environment

Fig. 13. Success rates of resilient consensus versus the  $R_0$  of SIR model and  $r$  in the regular agents

environment, we set the infected agents to be all near the agent that has the minimum degree.

We test the proposed static policy without the theoretical connectivity conditions given in (19)–(22). Instead, the policy maker chooses  $b_0 = b^*$  and the regular agents choose  $F_{i0} = \lceil (1 - b_0) \frac{n}{2} \rceil$ . Similarly, for the dynamic policy, the regular agents use (8) and  $F_i(k) = \lceil (1 - b(k)) \frac{n}{2} \rceil$ . The parameters in (23) are not met. We test these two policies in both homogeneous infected environment and gathered infected environment. The heatmaps representing the success rates of resilient consensus are displayed in Fig. 12 for  $(R_0, r) \in [1, 20] \times [0, 150]$ .

We first discuss the results for the static policy. As shown in Figs. 12(a) and 12(b), for dense network ( $r > 100$ ), the static policy works for almost any  $R_0 \in [1, 20]$ . This is in alignment with what we have shown in Section IV. From this simulation, we can also see that in dense networks, the static policy works in a wide range of  $R_0$ . For sparse networks ( $r < 50$ ), we can see that the static policy works with limited  $R_0$ . The results also show that the proposed static policy works similarly in both homogeneous infected environment and gathered infected environment. The reason is that we chose  $F_{i0} = \lceil (1 - b_0) \frac{n}{2} \rceil$ , which is based on the worst case analysis. When the network connection is satisfied so that all agents have enough neighbors, even the gathered infectious distribution is a minor part so that  $F_{i0} > I(k)d_i, \forall i, k$ . Similar explanations can also apply to the dynamic policy results.

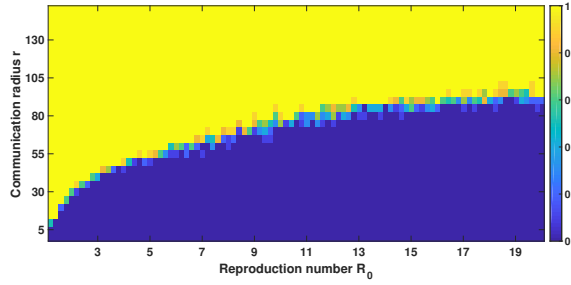
We choose another local static policy for comparison. The policy maker chooses  $b_0 = b^*$  while the regular agents in this case can set their pruning number individually according to the number of their neighbors as  $F_{i0} = \lceil (1 - b_0) \frac{d_i}{2} \rceil$ . Compared to the local policy discussed above, this local version may be

less resilient since the pruning number is smaller in general when the number of infected neighbors is large. The heatmaps for homogeneous and gathered environments are displayed in Fig. 13. From the result in Fig. 13(a), it is easy to see the effects of homogeneous condition. In a homogeneous environment, the policy works well in a wide range of  $R_0$  and communication radius ( $r \geq 80$ ). Compared with the worst case static policy, this algorithm requires less connection. The reason comes from the homogeneous condition. Within the sparse network, the part that has limited neighbors must have fewer infected nodes. The regular agents in such areas may remove less neighbors since  $F_{i0} = \lceil (1 - b_0) \frac{d_i}{2} \rceil$  and  $d_i$  is small. For the same network, if we apply the worst case policy, such regular agents may not have enough neighbors since  $F_{i0} = \lceil (1 - b_0) \frac{n}{2} \rceil$ . However, as shown in Fig. 13(b), in the gathered infection environment, the proposed local static policy is effective for fewer networks ( $r > 120$ ). Since in the gathered areas, regular agents use the pruning number smaller than  $I_{\max}n$ , the agents fail to reach resilient consensus.

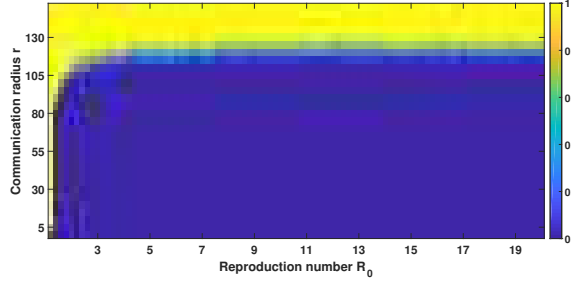
In the next simulation, we would like to show another local dynamic policy by choosing (8) and  $F_i(k) = \lceil (1 - b(k)) \frac{d_i}{2} \rceil$ . The heatmaps for homogeneous and gathered environments are displayed in Fig. 14. Clearly, they have similar profiles as the local static policy and the related arguments also hold here.

#### D. Time Response for the Proposed Two Policies

In this last part of simulations, we check the time responses for the proposed static and dynamic policies. For this part, a small random network with 100 nodes is chosen in the area of  $100 \times 100$ . The communication radius is 100. The initial SIR ratio is  $S(0) = 0.99, I(0) = 0.01$ , and  $R(0) = 0$ . The



(a) Local dynamic policy within homogeneous infection environment



(b) Local dynamic policy within gathered infection environment

Fig. 14. Success rates of resilient consensus versus the  $R_0$  of SIR model and  $r$  in the regular agents

sampling period is  $\Delta T = 0.01$ . Susceptible and recovered agents randomly take initial values from  $[0, 1]$ , which is considered as the safety interval. Once an agent is infected, its value is changed to  $-1$  by the disease. The infected agents are randomly chosen, and hence the homogenous condition is not guaranteed. The time responses for the two cases with  $R_0 = 5, r = 70$  and  $R_0 = 5, r = 100$  are shown in Fig. 15. We place the curves of  $S(k), I(k), R(k)$  in the plots so that the real time infectious situation is clear. Here, we also plot the ratio of the agents taking negative numbers in the system. Under normal situations, this ratio should match that of the infected agents since the recovered agents will attain states within the safe interval shortly after their recovery. However, under severe conditions when the recovered agents have too many infected neighbors, this ratio may grow over time. We will see that a phase transition where this ratio becomes 1 can happen.

We first look at the proposed static and dynamic policy, shown in Figs. 15(a), 15(b), 15(c), and 15(d). We can see that both policies guarantee resilient consensus and the infected values are almost all coming from the infected agents. To compare the static and dynamic policies with the same  $R_0$ , the result shows that the dynamic policy has an earlier infectious peak. At the beginning, when  $I(k)$  is low, the dynamic policy usually has fewer pruning numbers so that the peak may appear earlier. However, the  $I_{\max}$  in the two policies is almost the same, which is also indicated in Fig. 4.

Then, we look at the results for local static and dynamic policy, which are shown in Figs. 15(e), 15(f), 15(g) and 15(h). Within the sparse network ( $r = 70$ ), both local static and dynamic policies fail to reach resilient consensus. The regular agents fail to keep healthy states when the infected agents

reach a certain level. Within the denser network ( $r = 100$ ), the local static policy reaches resilient consensus, but the local dynamic policy fails. These results indicate that for both local static and dynamic policies, the homogenous condition is important for reaching resilient consensus. Moreover, compared with the local static policy, the local dynamic policy is more fragile since they remove less neighbor values. Once there is any agent who has more than  $I(k)d_i/2$  infected neighbors, unsafe values dominate the agents, indicating that consensus is reached but it is not resilient.

Next, we would like to show how the initial SIR ratios affect the performance of proposed two policies. We slightly changed the SIR ratios to  $S(0) = 0.9, I(0) = 0.1, R(0) = 0$  and generated the time responses for all policies. The results are shown in Fig. 16. From the results in Figs. 16(a) and 16(c), we can see both the static policy and the local static policy fail to reach resilient consensus even within the dense network ( $r = 100$ ). The reason for the failure under the static policy comes from the approximate calculation for  $I_{\max}$  in (11), where  $S(0) \approx 1, I(0) \approx 0$  are assumed. Here, we found that the initial ratios used here  $S(0) = 0.9, I(0) = 0.1, R(0) = 0$  do not satisfy the assumption so that the calculated  $b = b^*$  does not match the real  $I_{\max}$ . When  $I(k)$  increases over a bound (in this simulation it is  $I(k) \geq 0.2$ ), there are more infected agents than the MSR algorithm is prepared for, preventing resilient consensus. On the other hand, for the dynamic policy, we do not have such an issue and the ratio of negative values reduced to zero together with the infectious ratio  $I(k)$  as shown in Fig. 16(b). We also found that if  $S(0) \geq 0.97, I(0) \leq 0.03, R(0) = 0$ , then the static policy can guarantee resilient consensus with  $R_0 = 5$ .

## VII. CONCLUSION

In this paper, we have considered resilient consensus problems in the presence of misbehaving agents, whose number changes according to the level of pandemic. Resilient protocols have been proposed to mitigate their influence on regular agents. Analyses have been made for both static and dynamic policies for the transmission reduction parameter. Moreover, we characterized the relation between graph conditions and the pandemic reproduction number. Numerical simulations further studied the theoretical and practical bound, homogeneous conditions and time responses of the proposed protocols in random graphs. Future directions include extending this study to other distributed epidemic models, developing other contacting reduce policies and so on.

## REFERENCES

- [1] H. J. Ahn and B. Hassibi, Global dynamics of epidemic spread over complex networks, In *Proc. 52th IEEE Conference on Decision and Control (CDC)*, pp. 4579–4585, 2013.
- [2] K. Ali, T. Başar, and B. Ghareisifard, Stability of epidemic models over directed graphs: A positive systems approach, *Automatica*, 74, pp. 126–134, 2016.
- [3] C. Briat and E.I. Verriest, A new delay-SIR model for pulse vaccination, In *IFAC Proc. Volumes*, 41(2), pp. 10295–10300, 2008.
- [4] S. Buhrman, J. A. Garay, and J. H. Hoepman. Optimal resiliency against mobile faults, In *Proc. 25th Int. Symp. Fault-Tolerant Computing*, pp. 83–88, 1995.

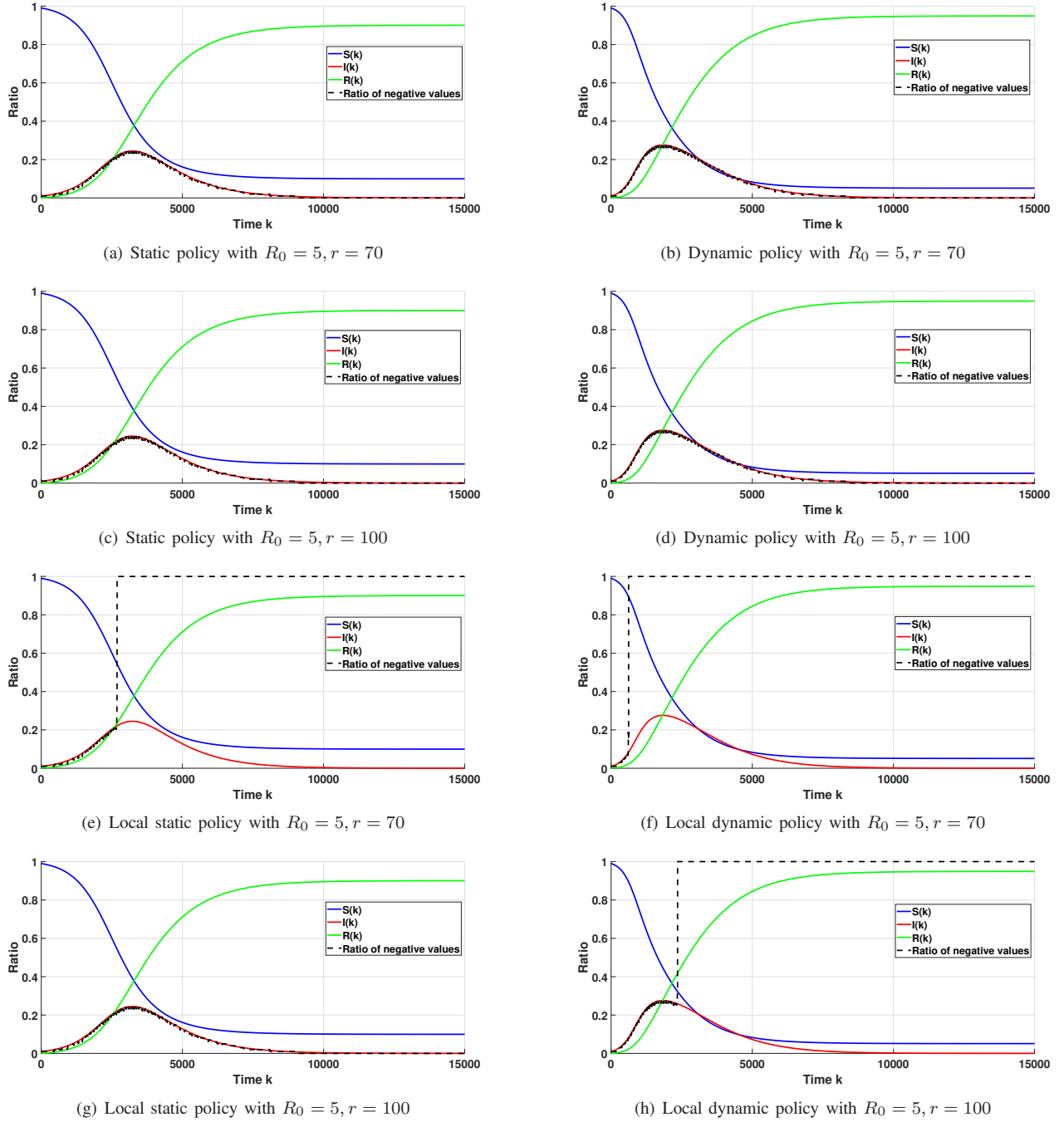


Fig. 15. Time responses for different policies with  $S(0) = 0.99, I(0) = 0.01, R(0) = 0$

- [5] Y. C. Chen, P. E. Lu, C. S. Chang, and T. H. Liu, Time-dependent SIR model for COVID-19 with undetectable infected persons, *IEEE Trans. Network Science and Engineering*, to appear, 2020.
- [6] Z. Chen, K. Zhu, and L. Ying, Detecting multiple information sources in networks under the SIR model, *IEEE Trans. Network Science and Engineering*, 36(1), pp. 17–31, 2016.
- [7] J. A. Garay, Reaching (and maintaining) agreement in the presence of mobile faults, In G. Tel and P. Vitányi (editors), *Distributed Algorithms WDAG 1994*, Lecture Notes in Computer Science, 857, Springer, 1994.
- [8] B. S. Graham, J. R. Mascola, and A. S. Fauci, Novel vaccine technologies: Essential components of an adequate response to emerging viral diseases, *JAMA*, 319(14), pp. 1431–1432, 2018.
- [9] A. R. Hota and S. Sundaram, Game-Theoretic vaccination against networked SIS epidemics and impacts of human decision-making, *IEEE Trans. Control of Network Systems*, 6(4), pp. 1461–1472, 2019.
- [10] D. Kempe, J. Kleinberg, and E. Tardos, Maximizing the spread of influence through a social network. In *Proc. ACM SIGKDD*, pp. 137–146, 2003.
- [11] W. O. Kermack and W. O. McKendrick, A contribution to the mathematical theory of epidemics. In *Proc. Royal Society of London, Series A*, 115(772), pp. 700–721, 1927.
- [12] F. D. Lauro, I. Z. Kiss, and J. Miller, The timing of one-shot interventions for epidemic control, *medRxiv*, doi: 10.1101/2020.03.02.20030007, 2020.
- [13] H. J. LeBlanc, H. Zhang, X. Koutsoukos, and S. Sundaram, Resilient asymptotic consensus in robust networks, *IEEE J. Selected Areas Comm.*, 31, pp. 766–781, 2013.
- [14] X. Li, C. Li, and X. Li, Minimizing social cost of vaccinating network SIS epidemics, *IEEE Trans. Network Science and Engineering*, 5(4), pp. 326–335, 2018.

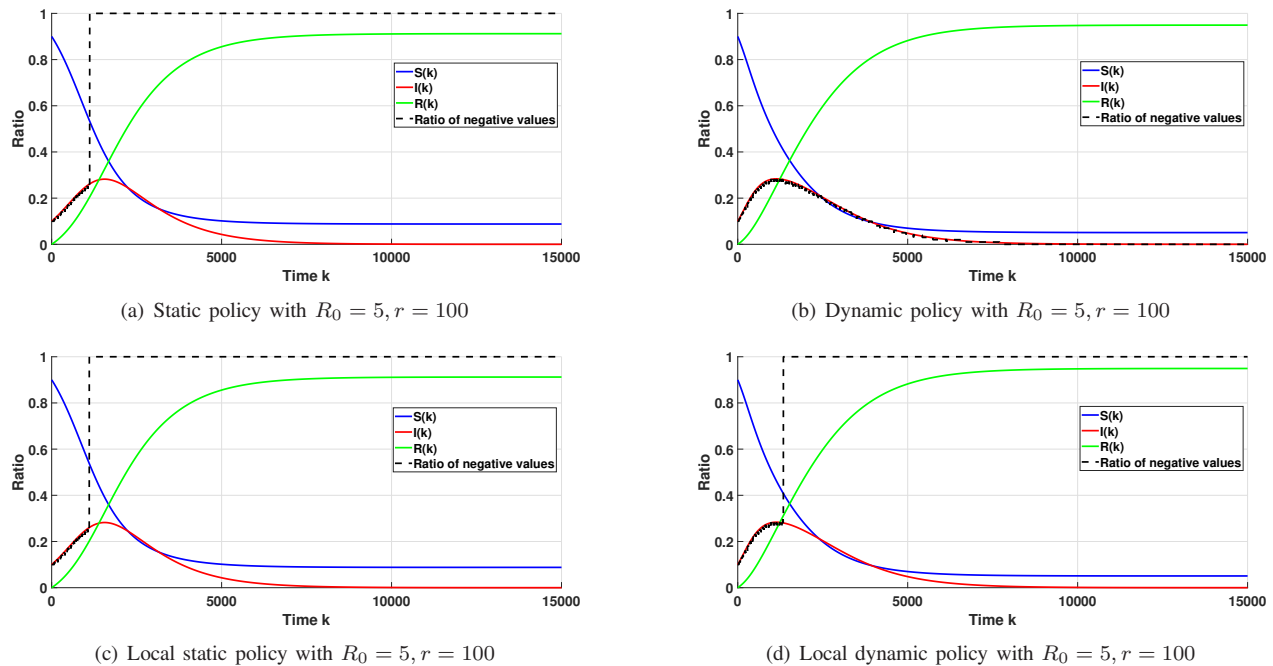


Fig. 16. Time responses for different policies with  $S(0) = 0.9, I(0) = 0.1, R(0) = 0$

- [15] F. Liu and M. Buss, Optimal control for heterogeneous node-based information epidemics over social networks, *IEEE Trans. Control of Network Systems*, 7(3), pp. 1115–1126, 2020.
- [16] V. S. Mai, A. Battou, and K. Mills, Distributed algorithm for suppressing epidemic spread in networks, *IEEE Control Systems Letters*, 2, pp. 555–560, 2018.
- [17] P. Van Mieghem, J. Omic, and R. Kooij, Virus spread in networks, *IEEE/ACM Transactions on Networking*, 17(1), pp. 1–14, 2009.
- [18] D. H. Morris, F. W. Rossine, J. B. Plotkin, and S. A. Levin, Optimal, near-optimal, and robust epidemic control, *arXiv:2004.02209v2*, 2020.
- [19] C. Nowzari, V. Preciado, and G. J. Pappas, Analysis and control of epidemics: A survey of spreading processes on complex networks, *IEEE Control Systems Magazine*, 36(1), pp. 26–46, 2016.
- [20] M. Ogura and V. M. Preciado, Efficient containment of exact SIR Markovian processes on networks. In *Proc. 55th IEEE Conference on Decision and Control (CDC)*, pp. 967–972, 2016.
- [21] R. Ostrovsky and M. Yung, How to withstand mobile virus attacks. In *Proc. ACM Symp. Principles of Distributed Comp.*, pp. 51–59, 1991.
- [22] P. E. Paré, C. L. Beck, and A. Nedić, Epidemic processes over time-varying networks, *IEEE Trans. Control of Network Systems*, 5(3), pp. 1322–1334, 2017.
- [23] P. E. Paré, J. Liu, C. L. Beck, B. E. Kirwan, and T. Basar, Discrete time virus spread processes: Analysis, identification, and validation, *IEEE Trans. Control Systems Technology*, 28(1), pp. 79–93, 2019.
- [24] B. Prasse and P. Van Mieghem, Network reconstruction and prediction of epidemic outbreaks for general group-Based compartmental epidemic models, *IEEE Trans. Network Science and Engineering*, 7(4), pp. 2755–2764, 2020.
- [25] V. M. Preciado, M. Zargham, C. Enyioha, A. Jadbabaie, and G. J. Pappas, Optimal resource allocation for network protection against spreading processes, *IEEE Trans. Control of Network Systems*, 1(1), pp. 99–108, 2014.
- [26] N. A. Ruhi and B. Hassibi, SIRS epidemics on complex networks: Concurrence of exact Markov chain and approximated models. In *Proc. 54th IEEE Conference on Decision and Control (CDC)*, pp. 2919–2926, 2015.
- [27] S. Trajanovski, Y. Hayel, E. Altman, H. Wang, and P. Van Mieghem, Decentralized protection strategies against SIS epidemics in networks, *IEEE Trans. Control of Network Systems*, 2(4), pp. 406–419, 2015.
- [28] S. Trajanovski, F. A. Kuipers, Y. Hayel, E. Altman, and P. Van Mieghem, Designing virus-resistant, high-performance networks: A game-formation approach, *IEEE Trans. Control of Network Systems*, 5(4), pp. 1682–1692, 2018.
- [29] N. H. Vaidya, L. Tseng, and G. Liang, Iterative approximate Byzantine consensus in arbitrary directed graphs. In *Proc. ACM Symp. Principles of Distributed Computing*, pp. 365–374, 2012.
- [30] D. Vrabac, P. E. Paré, H. Sandberg, and K. H. Johansson, Overcoming challenges for estimating virus spread dynamics from data. In *Proc. 54th Conf. Information Sciences and Systems*, pp. 1–6, 2020.
- [31] Y. Wan, S. Roy, and A. Saberi, Network design problems for controlling virus spread. In *Proc. 46th IEEE Conference on Decision and Control (CDC)*, pp. 3925–3932, 2007.
- [32] Y. Wang, H. Ishii, F. Bonnet, and X. Défago, Resilient consensus against mobile malicious agents. In *Proc. IFAC World Congress*, *arXiv:2006.11711*, 2020.
- [33] Y. Wang, H. Ishii, F. Bonnet, and X. Défago, Resilient consensus against epidemic malicious agents. In *Proc. European Control Conference*, to appear, 2021, also, *arXiv:2012.13757v1*.
- [34] N. J. Watkins, C. Nowzari, and G. J. Pappas, Robust economic model predictive control of continuous-Time epidemic processes, *IEEE Trans. Automatic Control*, 65(3), pp. 1116–1131, 2020.

PLACE  
PHOTO  
HERE

**Yuan Wang** (M'19) Yuan Wang received the M.Sc. degree in engineering from Huazhong University of Science and Technology, Wuhan, China in 2016, and the Ph.D. degree in Artificial Intelligence from Tokyo Institute of Technology, Yokohama, Japan in 2019. He is currently a researcher in the Division of Decision and Control Systems, KTH Royal Institute of Technology, Stockholm, Sweden.

His main research interests are cyber-physical systems, event-based coordination, security in multi-agent systems, and model predictive control methods.

PLACE  
PHOTO  
HERE

**Hideaki Ishii** (M'02-SM'12-F'21) received the M.Eng. degree in applied systems science from Kyoto University, Kyoto, Japan, in 1998, and the Ph.D. degree in electrical and computer engineering from the University of Toronto, Toronto, ON, Canada, in 2002. He was a Postdoctoral Research Associate with the Coordinated Science Laboratory at the University of Illinois at Urbana-Champaign, Urbana, IL, USA, from 2001 to 2004, and a Research Associate with the Department of Information Physics and Computing, The University of Tokyo, Tokyo, Japan, from 2004 to 2007. Currently, he is an Associate Professor in the Department of Computer Science, Tokyo Institute of Technology, Yokohama, Japan. His research interests are in networked control systems, multiagent systems, cyber security of power systems, and distributed and probabilistic algorithms.

Dr. Ishii has served as an Associate Editor for the *IEEE Control Systems Letters* and the *Mathematics of Control, Signals, and Systems* and previously for *Automatica*, the *IEEE Transactions on Automatic Control*, and the *IEEE Transactions on Control of Network Systems*. He is the Chair of the IFAC Coordinating Committee on Systems and Signals since 2017. He received the IEEE Control Systems Magazine Outstanding Paper Award in 2015.

PLACE  
PHOTO  
HERE

**François Bonnet** François Bonnet is a Specially Appointed Associated Professor at Tokyo Tech since 2018.

He obtained his M.S. from the ENS Cachan at Rennes, France in 2006 and his Ph.D. from the University of Rennes 1 in 2010. He worked at JAIST as a JSPS postdoctoral fellow until 2012 and then as an Assistant Professor until 2017. Then he spent one year as a Specially Appointed Assistant Professor at Osaka University.

His research interests include theoretical distributed computing, discrete algorithms, and (combinatorial) game theory.

PLACE  
PHOTO  
HERE

**Xavier Défago** (M'93) Xavier Défago is a full professor at Tokyo Institute of Technology since 2016.

He obtained master (1995) and PhD (2000) in computer science from the Swiss Federal Institute of Technology in Lausanne (EPFL) in Switzerland. Before his current position at Tokyo Tech, he was a faculty member at the Japan Advanced Institute of Science and Technology (JAIST). Meanwhile, he has also been a PRESTO researcher for the Japan Science and

Technology Agency (JST), and an invited researcher for CNRS (France) at Sorbonne University and at INRIA Sophia Antipolis.

He is a member of the IFIP working group 10.4 on dependable computing and fault-tolerance. He served as program chair of IEEE SRDS in 2014 and IEEE ICDCS in 2012 and as general chair of SSS 2018.

Xavier has been working on various aspects of dependable computing such as distributed agreement, state machine replication, failure detection, and fault-tolerant group communication in general. His interest include also robotics, embedded systems, and programming languages.